A sensor for the direct measurement of curvature based on flexoelectricity

2013 Smart Mater. Struct. 22 085016

(http://iopscience.iop.org/0964-1726/22/8/085016)

Smart Mater. Struct. **22** (2013) 085016 (8pp) doi:10.1088/0964-1726/22/8/085016

A sensor for the direct measurement of curvature based on flexoelectricity

Xiang Yan, Wenbin Huang, Seol Ryung Kwon, Shaorui Yang, Xiaoning Jiang and Fuh-Gwo Yuan

Department of Mechanical and Aerospace Engineering, North Carolina State University, Raleigh, NC 27695, USA

E-mail: yuan@ncsu.edu

Received 16 December 2012, in final form 15 June 2013
Published 11 July 2013
Online at stacks.iop.org/SMS/22/085016

Abstract
A direct curvature sensing measurement based on the flexoelectricity of $Ba_{0.64}Sr_{0.36}TiO_3$ (BST) material through electromechanical coupling is proposed and developed in this paper. The curvature sensing was demonstrated in four point bending tests of a beam with bonded BST curvature sensors under different applied loads with low time-harmonic frequencies from 0.5 to 3 Hz. A shear lag concept which describes the efficiency of the loading transfer from the epoxy bonding layer was taken into account in extracting the actual curvature from the sensor measurement. A finite element analysis has been performed to estimate the curvature transfer efficiency and the bonding layer thickness is found to be a critical parameter in determining the curvature transfer. Experimental results showed a good linearity of charge output dependence on curvature inputs in a limited frequency range and showed a curvature sensitivity of 30.78 pC m, in comparison with 32.48 pC m from theoretical predictions. Using the measured curvature, the bending stiffness of the beam was then obtained from the experimentally obtained moment–curvature curve. This work demonstrated that the flexoelectric BST sensor provides a direct curvature measurement instead of using a traditional strain gage sensor through interpolation, and thus offers an important avenue for *on-line* and *in situ* structural health monitoring.

(Some figures may appear in colour only in the online journal)

1. Introduction

The 'curvature' of loaded structures is always of interest in the field of the strength of materials and structures. However, in practice this physical parameter is difficult to measure directly. It is known that the structural curvature and material strain are functionally related and one can usually be inferred from knowledge of the other. Therefore, material strain has traditionally been measured to indicate the amount of structure deformation or loading [1] and there are numerous commercially available strain sensing devices that can be used to measure strain. However, strain measurement is not necessarily the best measurand in monitoring curvature. For example, plate-like thin elements are frequently used in modern infrastructure and aerospace structures. The strain is proportional to the thickness of the structure, and the strain magnitude decreases with decrease in structural thickness under fixed curvature, leading to difficult strain measurements. In contrast, curvatures are constant throughout any structural section because the structural thickness is several orders of magnitude smaller than the radius of the curvature. Therefore, curvature measurements can be performed anywhere in a cross section, including the neutral plane, even where there is no strain under pure bending [2]. Thus, there is a need for direct measurement of curvature, instead of indirect strain measurement, for health monitoring of thin slender structures [3].

In the field of structural health monitoring, structural damage is usually reflected by a change in the stiffness of structures. Therefore, the use of sensors mounted on the structure to detect structural stiffness changes due to cracks or damage developed at or away from the sensor location [4] is very desirable. However, existing sensing technology (e.g. strain gages, accelerometers, linear voltage displacement

transducers) accompanied by interpretation algorithms is not effective for *in situ* monitoring of early damage because of its limited sensitivity, bandwidth, and accessibility to the hidden localized areas, let alone damage initiation and progression [5]. Apart from the above sensing technology, if a sensor located at any location across the cross section can measure curvature directly, the sensor will provide an indication of any change in the stiffness of a structure subject to bending. Consequently, curvature sensors may be attractive for applications in structural integrity monitoring, such as bridges, or structural components of aircraft.

To date, sensors that can measure curvature have rarely been reported. The first documented sensor, called a 'curvature gage', that could measure curvature was a fiber-optic sensor proposed by Djordjevich and Boskovic in 1996 [1]. Since a bend in the fiber affects the output light intensity, the curvature can be measured by the output light intensity. 'Fiber-optic' based curvature sensors have since been studied extensively by many researchers [2, 3, 6–12]. Although most of the reported fiber-optic based curvature sensors have advantages such as immunity to electromagnetic interference, corrosion resistance, and large bandwidth [7], the complexity of the measurement system using a power supply required to provide the light source, a non-smooth fiber surface needed to increase sensitivity, and a complicated operation principle, has prohibited its practical engineering applications. In addition to fiber-optic curvature sensors, an inexpensive conductive ink sensor that can detect curvature with relatively lower measurement range was reported in [13]. The wavelength-shift technique and the light interferometric technique can also be used to measure bending curvature [14, 15], but these systems are complex and expensive.

In this paper, a novel flexoelectric BST ceramic curvature sensor is proposed, for the first time, to measure bending curvature directly. It is studied theoretically and is tested experimentally by attaching the sensor to the side surface of an aluminum beam under four point bending conditions to sense the beam curvature when the load monotonically increases. The main features of the flexoelectric curvature sensor reported include direct curvature measurement, low frequency range applicability, high sensitivity, and no external excitation source needed. The flexoelectric curvature sensor is an alternative to strain measurement and is capable of *on-line* and *in situ* structural integrity monitoring.

The paper is organized as follows. After the introduction, section 2 presents the curvature sensor design, where beam curvature, flexoelectricity, fabrication of the curvature sensor and beam curvature sensing are discussed in detail. Section 3 illustrates the experimental procedures and results. Section 4 discusses the major findings of this paper and provides recommendations for future investigations, followed by conclusions.

2. Curvature sensor design

2.1. Beam curvature

The simplest test system to introduce curvature is a four point bending beam, the set-up of which is shown in figure 1.

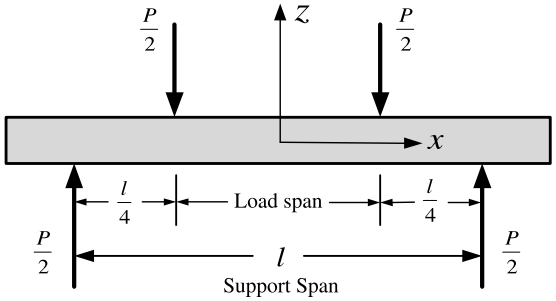

Figure 1. Loading diagram for four point bending (ASTM standard).

In the pure bending mid-section, which is the load span shown in the figure, the bending moment and axial strain can be given as

$$M = \frac{P}{2}\frac{l}{4}, \tag{1}$$

$$\varepsilon_x = \frac{M}{EI}z = \frac{3Pl}{2Ebh^3}z, \tag{2}$$

where M is the bending moment and ε_x is the normal strain along the x direction. From simple beam bending theory, the curvature ($\kappa = 1/R$) is related to the bending moment (M) via the bending stiffness (EI), as given by the Euler bending formula

$$\kappa = \frac{M}{EI} = \frac{\mathrm{d}\varepsilon_x}{\mathrm{d}z} = \frac{3Pl}{2Ebh^3}, \tag{3}$$

where $\mathrm{d}\varepsilon_x/\mathrm{d}z$ is the strain gradient through the thickness direction. It can be easily seen that if a sensor could respond to beam strain gradient (curvature), it would be a viable candidate for curvature sensing.

2.2. Flexoelectricity

In a piezoelectric material such as lead zirconate titanate (PZT), an applied uniform load (strain) can generate electric polarization or vice versa. This piezoelectric effect (figure 2(a)) is well recognized and has been exploited extensively in a broad field for both sensing and actuation applications. In crystallography, non-centrosymmetry is a necessary condition for crystal systems (20 out of 32 point groups) to exhibit piezoelectricity. Flexoelectricity (FE) is, however, the coupling between the mechanical strain gradient and the electric polarization (figure 2(b)). It is the result of the non-uniform strain or strain gradient that can locally break inversion symmetry and induce charges even in centrosymmetric crystals. Thus, FE exists in all insulated solids. This opens up a broader choice of materials including lead and non-lead dielectrics with preferable properties [16]. In 1964, Kogan [17] first discussed the electric polarization induced in a centric crystal by inhomogeneous deformation and proposed the electromechanical coupling relationships of FE, which can be described as

$$P_l = \mu_{ijkl}\frac{\partial \varepsilon_{ij}}{\partial x_k}, \tag{4}$$

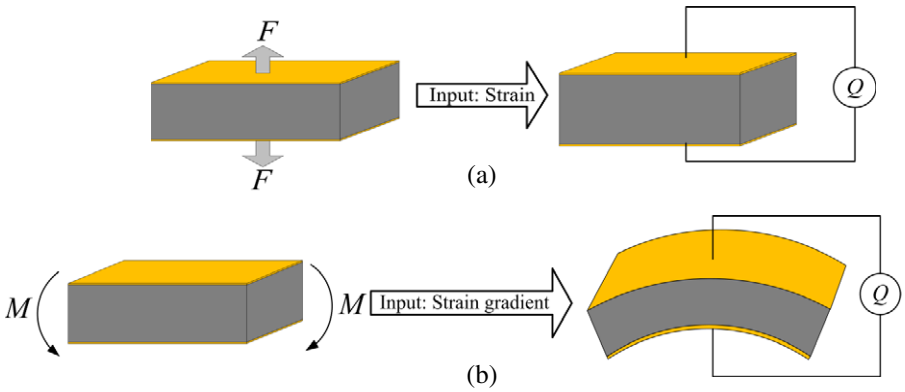

Figure 2. (a) The direct piezoelectric effect and (b) the direct flexoelectric effect.

Table 1. Material and geometric properties of BST.

Symbol	Description	Value	Units
ρ	Mass density	8200	kg m^{-3}
E	Young's modulus	153	GPa
ν	Poisson's ratio	0.33	—
l_s	Length	5	mm
b_s	Width	1	mm
h_s	Thickness	0.4	mm

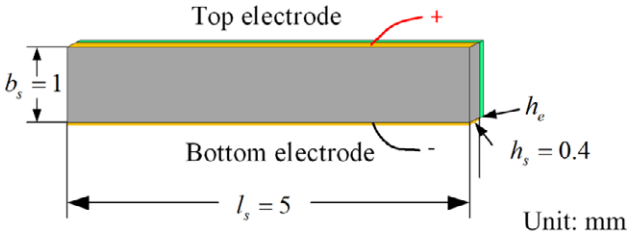

Figure 3. Curvature sensor configuration.

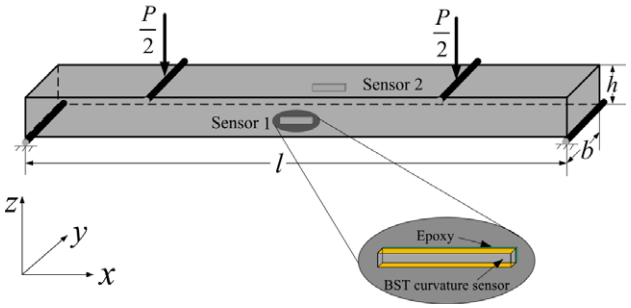

Figure 4. Beam curvature sensing: BST curvature sensor attached to a beam.

where P_l is the flexoelectric polarization, μ_{ijkl} is the flexoelectric coefficient, ε_{ij} is the elastic strain, and x_k is the position coordinate. μ_{ijkl} is a fourth-rank polar tensor and therefore has nonzero components μ_{1111}, μ_{1122}, μ_{2323}, or in matrix contracted notation μ_{11}, μ_{12}, μ_{44}, in a cubic crystal. Kogan also suggested an estimation of the order of magnitude of the flexoelectric coefficient as $\mu_{ijkl} \approx e/a$, where e is the charge of the electron and a is the atomic dimension of the unit cell of the dielectric. Phenomenological arguments indicated that this value for normal dielectrics should be multiplied by the relative permittivity for the case of high permittivity materials including ferroelectrics [18]. Ma and Cross [19] confirmed the theory experimentally and showed that the flexoelectric coefficients in ferroelectric materials are many orders of magnitude higher (10^{-6}–10^{-4} C m^{-1}) than that in simple dielectrics ($\sim 10^{-10}$ C m^{-1}). Therefore, ferroelectric materials with high permittivity can be deployed as flexoelectric materials in a curvature sensor for curvature sensing.

2.3. Fabrication of the curvature sensor

At present, $Ba_xSr_{1-x}TiO_3$ (BST) ceramic presents the highest flexoelectric coefficients among all reported ferroelectric materials [20]. In this study, curvature sensors were fabricated using BST ceramic with the composition of Ba:Sr = 64%:36%, which was laboratory-prepared using a conventional solid state processing method. The Curie temperature of the prepared BST samples was about 18 °C and the relative dielectric constant at room temperature was about 14 000. Impedance analysis of the BST ceramic showed no resonant or anti-resonant frequency in the frequency range of 40 Hz–110 MHz at room temperature, which means that the prepared BST samples were pure flexoelectric and did not have piezoelectricity at room temperature. The transverse flexoelectric coefficient μ_{12} of the prepared BST samples was measured to be about 28 μC m^{-1} using the cantilever measurement method developed in [21]. Other material properties and dimensions of the BST sensor are listed in table 1.

Figure 3 shows schematically the curvature sensor with electrodes on the top and bottom surfaces (5 mm × 0.4 mm). h_e is the thickness of the epoxy bonding layer.

2.4. Beam curvature sensing

The small size and light weight BST sensors can be attached to any location on a beam and exert little impact on the host structure. In order to capture the beam curvature, two BST curvature sensors were attached to the center of the side surfaces of an aluminum beam, located symmetrically with respect to its neutral axis, as illustrated in figure 4. The sensor

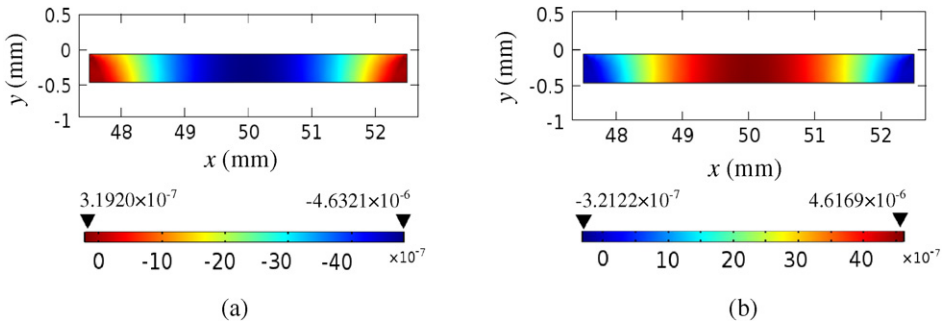

Figure 5. Average strain distribution (color bar) on (a) the top and (b) the bottom surface of the curvature sensor.

Table 2. Material and geometric properties of aluminum.

Symbol	Description	Value	Units
ρ	Mass density	2700	kg m^{-3}
E	Young's modulus	73	GPa
ν	Poisson's ratio	0.33	—
l	Length	0.1	m
b	Width	0.05	m
h	Thickness	0.0127	m

captures the beam curvature through strain gradient transfer through the bonding epoxy. Coaxial wires were bonded to the top and bottom electrodes using silver paste to eliminate external noise. The positive wire was connected to the top electrode, while the ground wire was attached to the bottom one. The beam material properties and geometry are shown in table 2.

Epoxy adhesive (Hysol EA 9359.3) was used to bond the BST curvature sensor to the aluminum beam. The shear modulus of the epoxy at room temperature is 1.03 GPa. A pressure of 0.2 MPa was applied to ensure uniform thickness of the epoxy layer h_e, which was measured to be about 60 μm using a microscope (Olympus STM6). The epoxy bonding layer is essential to insulate the electrodes from the metal beam. In addition, the epoxy bonding layer bridges the beam curvature (strain gradient) to the BST sensor for curvature measurement. The efficiency of the load transfer from the beam to the sensor through the epoxy is usually characterized by the curvature transfer coefficient caused by the shear lag effect [22, 23].

A static FEM model is established to calculate the curvature transfer coefficient. The model considered is to apply a 500 N force to a four point bending aluminum beam with a BST sensor attached. Under this load, a 6.25 Nm moment introduces a 0.01 m^{-1} beam curvature generated in the pure bending area of the beam. Figure 5 shows the average strain distribution on the top and bottom surfaces of the curvature sensor. The estimated average strain values $\bar{\varepsilon}_x$ on the top and bottom surfaces are calculated as $-2.90\ \mu\varepsilon$ and $2.88\ \mu\varepsilon$, respectively. Then, the average sensor strain gradient can be approximated by

$$\left(\frac{\partial \varepsilon_x^s}{\partial z}\right)_{av} = \frac{\bar{\varepsilon}_{x_{bottom}} - \bar{\varepsilon}_{x_{top}}}{b_s}, \tag{5}$$

where b_s is the thickness of the BST sensor. Therefore, the curvature transfer coefficient η can be calculated by

$$\eta = \frac{\left(\frac{\partial \varepsilon_x^s}{\partial z}\right)_{av}}{\kappa}. \tag{6}$$

By substituting equation (5) into equation (6), the curvature transfer coefficient is calculated as 0.582, which means that only 58.2% of the actual beam curvature is transferred from the aluminum beam to the curvature sensor through the bonding layer.

With the transferred strain gradient, the generated average polarization P_3 in the curvature sensor induced by the FE effect can be approximated from equation (4) by

$$P_3 = \mu_{12}\left(\frac{\partial \varepsilon_x^s}{\partial z}\right)_{av}, \tag{7}$$

where $(\partial \varepsilon_x^s/\partial z)_{av}$ is the average sensor strain gradient and the electric displacement D_3 is equal to the polarization density P_3 in this case. Finally, combining equations (6) and (7), the total average charge Q accumulated in the electrode can be written as

$$Q = \int_{A_e} D_3 dA = \int_{A_e} \mu_{12}\left(\frac{\partial \varepsilon_x^s}{\partial z}\right)_{av} dA = \mu_{12}\eta\kappa A_e, \tag{8}$$

where A_e is the area of the electrode.

To investigate how the thickness of the epoxy bonding layer affects the curvature transfer, a parametric study is performed using the same finite element model established above by changing the thickness of the bonding layer from zero to the thickness of the BST sensor. Figure 6 shows the relationship between the curvature transfer coefficient and the ratio of the epoxy bonding layer thickness to the BST sensor thickness. It is seen from the figure that the curvature transfer coefficient increases as the thickness of the epoxy bonding layer decreases, and thus the charge output (equation (8)) of the sensor increases as well. Therefore, the thickness of the epoxy bonding layer plays a critical role in determining the sensor charge output.

3. Experimental results

Four point bending tests were conducted on an aluminum beam using a hydraulic tester (Instron model 1331), as shown

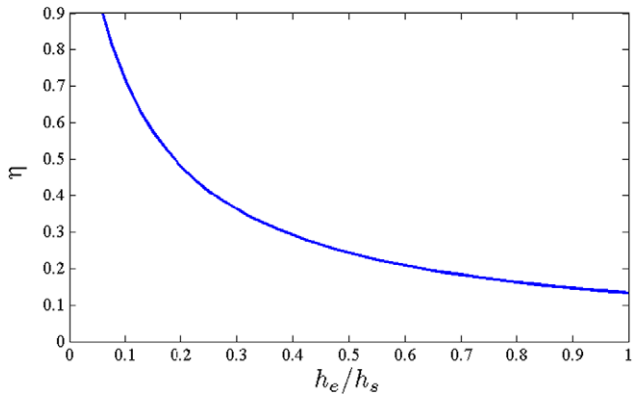

Figure 6. Relationship between the curvature transfer coefficient and the ratio of the epoxy bonding layer thickness to the BST sensor thickness.

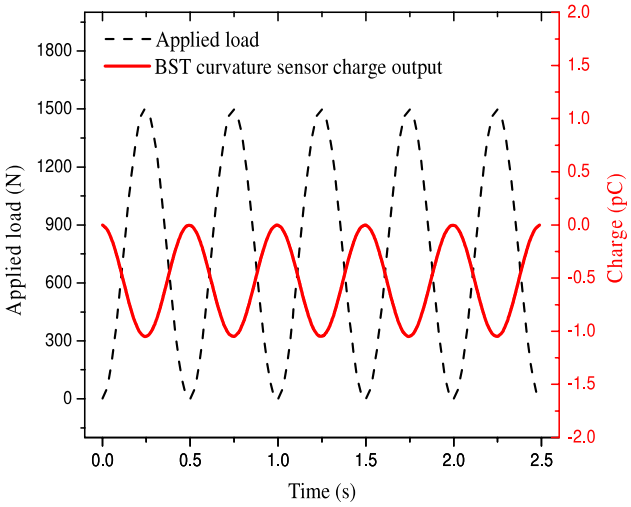

Figure 8. Real time charge output from BST sensor 1.

in figure 7. Two BST curvature sensors were attached to the two opposite side surfaces at the center of the beam. The load applied to the bending fixture was monotonically increased from 1.5 to 11.5 kN. The experiments were repeated three times for each sensor in the low frequency range, from 0.5 to 3 Hz with increments of 0.5 Hz, and the BST curvature sensors exhibited good repeatability. The charge output of the BST sensor was monitored using a charge amplifier and was then displayed and recorded in an oscilloscope (Agilent DSO7104B). Sensor sensitivity and the moment–curvature relationship are discussed in detail in the following two sub-sections.

3.1. Charge output and sensor sensitivity

Figure 8 shows the real time charge output of BST sensor 1 under a sinusoidal load with a peak-to-peak value of 1500 N at 2 Hz, and it can be observed that the charge output is out-of-phase with the applied load. This is because the beam is bent downward causing the strain gradient direction of the BST sensor to be opposite to the wire connection. It is also found from the experiments that both the BST sensors exhibit similar responses, as shown in figure 8, and the charge outputs from both BST sensors remain the same with the frequency varying within 0.5–3 Hz under the same applied load. Thus, the charge output of the BST sensor is frequency independent in this low frequency range. The charge outputs of both the BST sensors with different applied loads within 0.5–3 Hz frequency range are listed in table 3. In the table, the moment, beam curvature and average sensor strain gradient are obtained from equations (1), (3) and (6), respectively. Figure 9 illustrates the relationship between the flexoelectric charge outputs of the BST sensors and the beam curvature. The solid line is the theoretical charge output calculated from equation (8) by taking into account the shear lag effect caused by the 60 μm thick bonding layer. The red dotted points are the actual charge outputs obtained from table 3 from both the BST sensors and with the standard deviation error bar added, which shows that only very minor charge output error appears among individual experiments. The slope of the charge output versus beam curvature can be defined as the sensitivity of the curvature sensor, with units of pC m. The experimental charge outputs of the curvature sensor show very good linearity with the beam curvature, and agree with the theoretical charge output predictions well. The experimental sensitivity of the curvature sensor is found to be 30.78 pC m, while the theoretical sensitivity is 32.48 pC m. From figure 9, the experimental charge outputs are a bit smaller than the

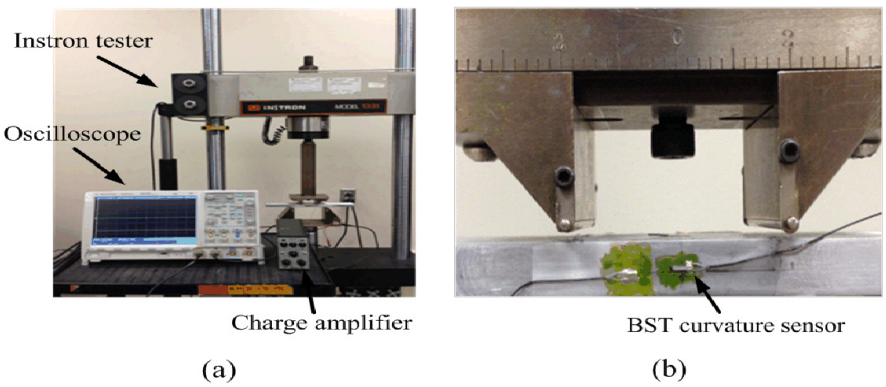

Figure 7. (a) Experimental set-up and (b) a close-up of the actual curvature sensor attached to the beam.

Table 3. Experimental charge outputs under different loads within a 0.5–3 Hz frequency range.

Applied load P (N)	Moment M (Nm)	Beam curvature M/EI (m^{-1})	Average strain gradient transferred to sensor (m^{-1})	Charge output Q (pC) (sensor 1)	Charge output Q (pC) (sensor 2)
1 500	18.75	0.030	0.0175	1.02 1.05 1.00	1.02 1.03 1.01
3 000	37.50	0.060	0.0349	2.03 2.10 2.01	2.05 2.12 2.07
6 000	75.00	0.120	0.0698	3.80 3.60 3.50	3.80 3.60 3.50
9 000	112.50	0.181	0.1047	5.70 5.30 5.40	5.70 5.50 5.40
11 500	143.75	0.231	0.1338	7.30 6.40 7.20	7.10 6.50 7.30

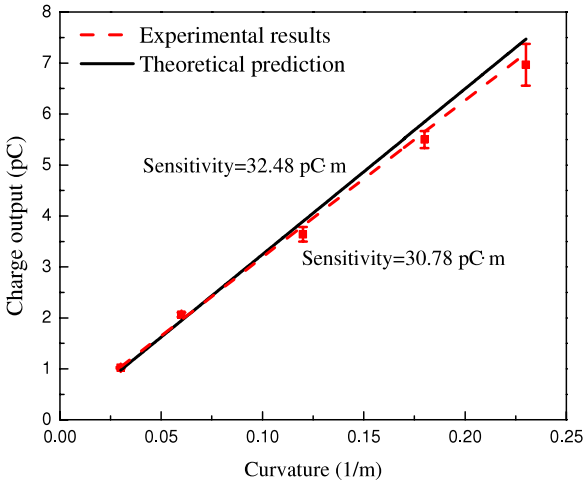

Figure 9. Relationship between charge output and beam curvature—experimental results.

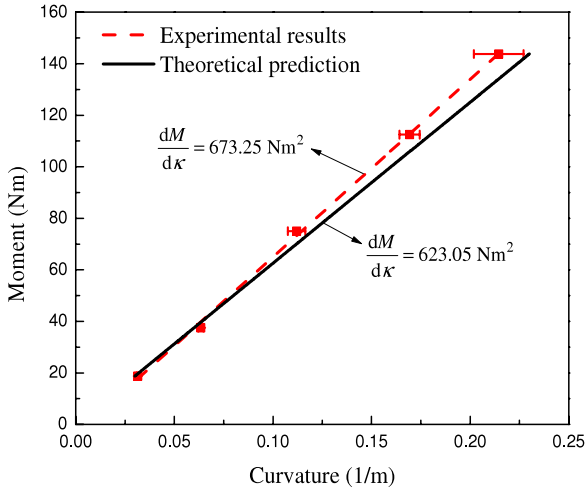

Figure 10. Moment–curvature relationship.

theoretical prediction and the slight discrepancy may come from several sources. The primary source of deviation may result from the actual thickness and uniformity of the adhesive bonding layer which can affect the effective curvature transfer. As the bonding layer thickness decreases, the curvature transfer becomes more effective, which in turn will increase the charge output, since the charge output is proportional to the curvature transfer efficiency. Therefore, if the thickness of the bonding layer is assumed to be less than 60 μm, there will be a better correlation between the experimental sensitivity and the theoretical prediction.

3.2. Moment–curvature relationship

The bending stiffness of a structural member can be measured from the moment–curvature relationship. $EI = M/\kappa$ shown in figure 10 presents the relationship between the moment and the curvature. With the experimental charge output shown in table 3, the beam curvature can be estimated from equation (8) by $\kappa = Q/(\eta\mu_{12}A_e)$, while the theoretical calculation of the beam curvature can be easily obtained from equation (3). The curvature of the beam ranges from 0.03 to 0.231 m^{-1} in these tests. The red dotted points are experimental beam curvatures that the curvature sensor sensed under different applied moments, and the curvature standard deviation error bars are also included. The experimental results show a good linearity between moment and curvature and agree with the theoretical estimation well. The black line is the theoretical moment–curvature relationship based on simple beam theory discussed in section 2.1. The bending stiffness can be obtained from the M–k curve by extracting the slope of the curve.

The theoretically calculated bending stiffness is 623.05 Nm^2 and the experimentally derived result is 673.25 Nm^2. The slightly discrepancy between the experimental and theoretical estimations of bending stiffness may be due to the thickness and non-uniformity of the bonding layer, as discussed above.

4. Discussion

The experimental results, which agreed with the theoretical predictions, demonstrate the feasibility of directly measuring curvature through electromechanical coupling of flexoelectricity. Control of the thickness of the epoxy bonding layer presents an important issue for the performance of the curvature sensor, and a bonding jig has been designed to better control the thickness and will be applied in future experiments. The sensors operate very well in lower frequency ranges; higher frequency performance remains to be investigated. The sensitivity of the sensor can be enhanced further by geometrically redesigning the sensor, e.g. bimorph or triple layer structure. The curvature range sensed for the tests is from 0.03 to 0.231 m^{-1}. Since the *M–k* curve exhibits very good linear behavior using the BST curvature sensor, in theory the BST curvature sensor can extend in response to smaller or larger curvature.

The beam bending stiffness obtained from the experimental moment–curvature relation can be used as an indicator of structural integrity. As the initiation of cracks and damage in structures often results in a reduction of stiffness, the BST curvature sensor, which can be attached at any location on the structure with little impact on the host structure, may hold promise for structural integrity monitoring.

Uniform distribution of curvature through the structural thickness gives an advantage of curvature measurement over strain measurement in thin structures, but this has raised a challenge for the size control of the curvature sensor. The BST sensor designed in this paper is suited to thin structural applications. Its size can be further reduced by using micro–nano fabrication techniques which will provide even wider applications for BST curvature sensing.

Besides, in comparison with the optical-fiber based curvature sensor, which requires a power supply for the light source, no external power sources are needed for the BST sensor because of its direct curvature sensing ability. The working principle of the BST sensor and the testing system are also much simpler than for the optical-fiber based curvature sensor.

5. Conclusions

The flexoelectric curvature sensor based on electromechanical coupling is the first reported sensor for direct measurement of the curvature. Flexoelectricity, which is the theoretical foundation of the BST curvature sensor, is discussed in detail. It is shown that the thickness of the bonding layer is critical for the sensor charge output and thus the sensitivity of the sensor. FEM analysis is used to quantify how efficiently the curvature is transferred from the structure to the sensor through the bonding epoxy layer due to the shear lag effect, and the thickness of the epoxy bonding layer is proven to be a critical parameter in determining curvature transfer efficiency. The fabrication and operating principle of the BST curvature sensor are also presented. Four point bending experiments have been conducted to test the performance of the curvature sensor in a low frequency range. The curvature sensor provides a sensitivity of 30.78 pC m in comparison with 32.48 pC m from theoretical prediction. Furthermore, the bending stiffness can be acquired from the beam moment–curvature relationship which is derived from the curvature sensor reading and is verified by Euler–Bernoulli beam theory.

The proposed curvature sensor offers conceptual and practical advantages over traditional strain measurements, especially for thin structures, so that the curvature sensor can provide higher sensitivity. The direct curvature reading and large sensing range of the BST curvature sensor make it feasible to sense any structural curvature. In addition, the non-embedded requirement of the sensor and the ability to monitor bending stiffness make it a promising sensing technique for structural health monitoring.

Acknowledgments

This material is based upon work supported in part by the US Army Research Laboratory and the US Army Research Office under contract/grant number W911NF-11-1-0516, and in part by the National Science Foundation under grant number CMMI-1068345.

References

[1] Djordjevich A and Boskovic M 1996 Curvature gauge *Sensors Actuators* A **51** 193–8
[2] Djordjevich A 2003 Alternative to strain measurement *Opt. Eng.* **42** 1888–92
[3] Kovačević M, Nikezić D and Djordjevich A 2004 Monte Carlo simulation of curvaturegauges by ray tracing *Meas. Sci. Technol.* **15** 1756–61
[4] Ma J J and Asundi A 2001 Structural health monitoring using a fiber optic polarimetric sensor and a fiber optic curvature sensor-static and dynamic test *Smart Mater. Struct.* **10** 181–8
[5] Farrar C R and Worden K 2007 An introduction to structural health monitoring *Phil. Trans. R. Soc.* A **365** 303
[6] Djordjevich A and He Y Z 1999 Thin structure deflection measurement *IEEE Trans. Instrum. Meas.* **48** 705–10
[7] Kovačević M, Djordjevich A and Nikezić D 2006 An analytical approach and optimization of curvature gauge *J. Phys.: Conf. Ser.* **48** 850858
[8] Djordjevich A 1998 Curvature gauge as torsional and axial load sensor *Sensors Actuators* A **64** 219–24
[9] Fu Y and Di H 2011 Fiber-optic curvature sensor with optimized sensitive zone *Opt. Laser Technol.* **43** 586–91
[10] Gong Y, Zhao T, Rao Y and Wu Y 2011 All-fiber curvature sensor based on multimode interference *IEEE Photon. Technol. Lett.* **23** 679–81
[11] Silva S, Frazao O, Viegas J, Viegas L A, Araujo F M, Malcata F X and Santos J L 2011 Temperature and strain-independent curvature sensor based on a singlemode/multimode fiber optic structure *Meas. Sci. Technol.* **22** 085201

[12] Zhang J, Liu H and Wu X 2009 Curvature optical fiber sensor by using bend enhanced method *Front. Optoelectron.* **2** 204–9
[13] Gentile C, Wallace M, Avalon T D, Goodman S, Fuller R and Hall T 1992 Angular displacement sensors *US patent* 5086785
[14] Wang Y, Chen J and Rao Y 2005 A novel long period fiber grating sensor measuring curvature and determining bend-direction simultaneously *IEEE Sensors J.* **5** 839–43
[15] Zhao S, Wang X and Yuan L 2008 Four core fiber based bending sensor *Front. Optoelectron.* **1** 231–6
[16] Tagantsev A K, Meunier V and Sharma P 2009 Novel electromechanical phenomena at the nanoscale: phenomenological theory and atomistic modeling *MRS Bull.* **34** 643–7
[17] Kogan S M 1964 Piezoelectric effect during inhomogeneous deformation and acoustic scattering of carriers in crystals *Sov. Phys. Solid State* **5** 2069–70
[18] Tagantsev A K 1986 The role of the background dielectric susceptibility in uniaxial ferroelectrics *Ferroelectrics* **69** 321–3
[19] Cross L E 2006 Flexoelectric effects: charge separation in insulating solids subjected to elastic strain gradients *J. Mater. Sci.* **41** 53–3
[20] Ma W H and Cross L E 2002 Flexoelectric polarization of barium strontium titanate in the paraelectric state *Appl. Phys. Lett.* **81** 3440–2
[21] Huang W B, Kim K, Zhang S J, Yuan F G and Jiang X N 2011 Scaling effect of flexoelectric (Ba, Sr)TiO_3 microcantilevers *Phys. Status Solidi RRL* **5** 350–2
[22] Crawley E F and de Luis J 1987 Use of piezoelectric actuators as elements of intelligent structure *AIAA J.* **25** 1373–85
[23] Sirohi J and Chopra I 2000 Fundamental understanding of piezoelectric strain sensors *J. Intell. Mater. Syst. Struct.* **11** 246–57